Electroweak measurements of multi-boson production with the ATLAS experiment

Speaker: Zhichen Wang

On behalf of the ATLAS group

Multi-boson measurements @ATLAS

Why measure multi-boson productions?

- Measurements of cross-section and polarization to validate the standard model (SM) at TeV scale
- Vector boson scattering/fusion (VBS/F) processes (with relative lower cross-section) to probe the mechanism of electroweak symmetry breaking
- Triple/Quartic Gauge boson coupling (T/QGC) to search for anomalous couplings and probe new physics
- Effective field theory (EFT) interpretation:

$$\mathcal{L}_{\mathrm{SMEFT}} \approx \mathcal{L}_{\mathrm{SM}}^{(4)} + \sum_i \frac{c_i^{(6)}}{\Lambda^2} O_i^{(6)} + \sum_j \frac{c_j^{(8)}}{\Lambda^4} O_j^{(8)}$$

- This presentation focuses on the diboson measurements with full ATLAS Run 2 data

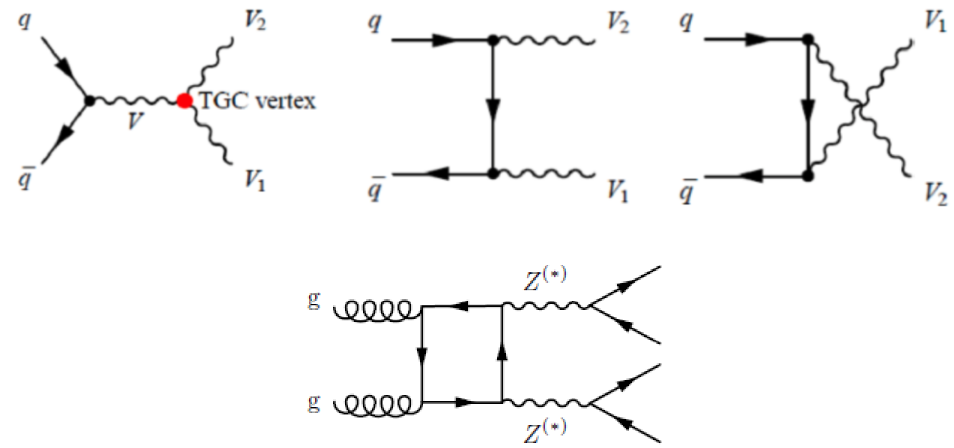

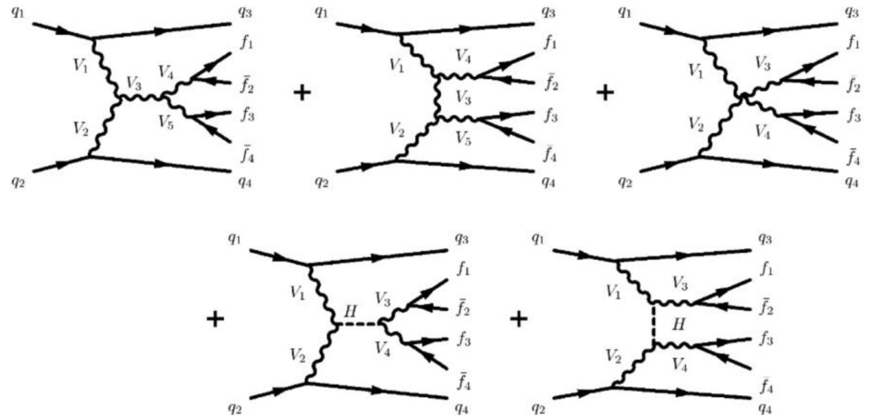

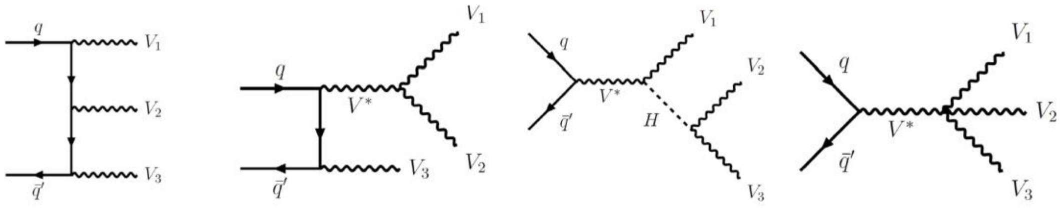

Overview

Measurements of diboson production

- EWK diboson (WW, WZ, ZZ) Arxiv
- EWK WZjj Arxiv
- ZZ Arxiv
- EWK Wγjj EPJC

Polarization study of diboson production

- WZ polarization Arxiv
- ZZ polarization Arxiv

Measurements of Triboson production:

- $WZ\gamma$ PRL
- $W\gamma\gamma$ inspire

Observation of the EWK diboson production

with a high-mass dijet system in semi-leptonic final states (Arxiv)

Signal: $(EWK)\ V_{lep}V_{had}jj$
Background: V+jets, $t\bar{t}$, single-t, (QCD) VV

One **leptonic** decayed V is reconstructed by 3 channels:
- 0-lepton
- 1-lepton
- 2-lepton

One **hadronic** decayed V is reconstructed by:
- 1 large-R jet (in merged selection)
- 2 small-R jets (in resolved selection)

Main signal

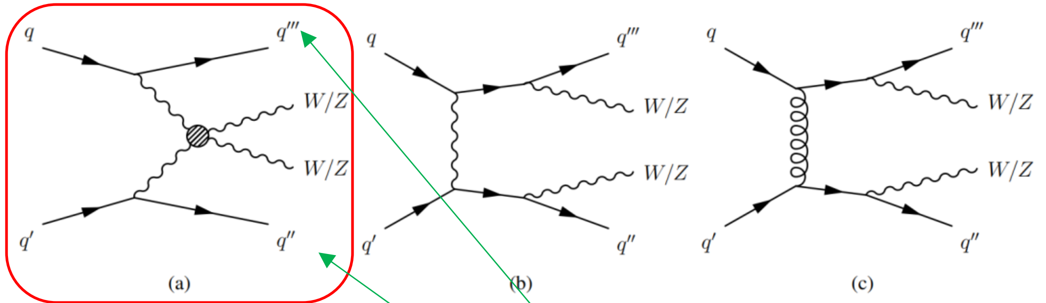

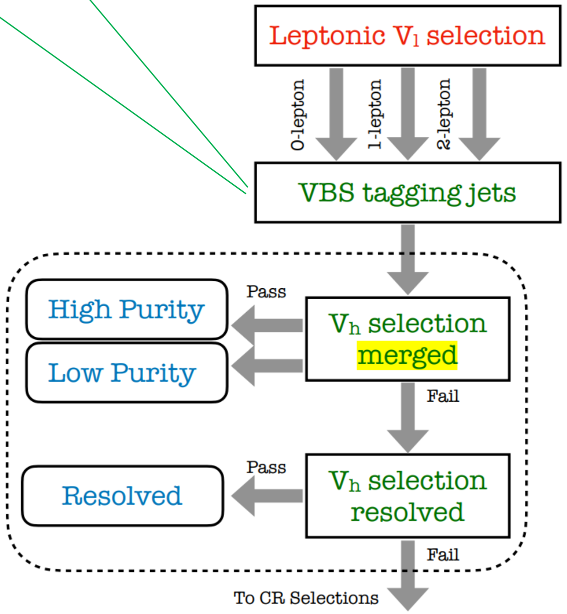

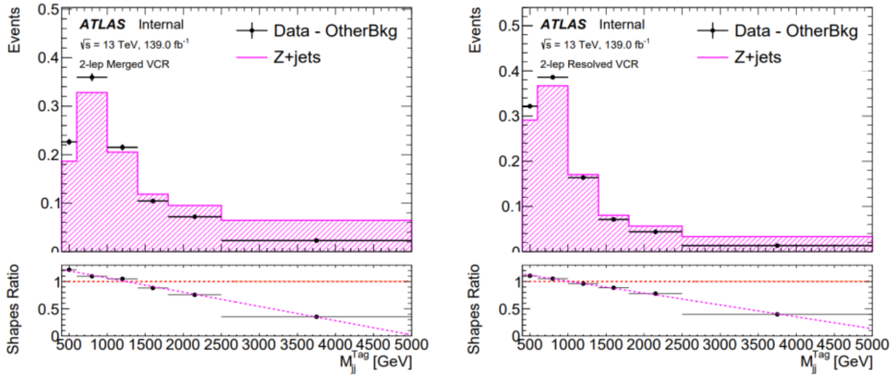

(a) (b)

V+jets CR (VCR): Same as SR except inverting one single cut represented by the mass cut (m_J, m_{jj})
$\boldsymbol{t\bar{t}}$ **CR** (**TCR**): Same as 1-lepton channel SR except the b-jet requirement is inverted
A data-driven reweighting is applied to W+jets and Z+jets samples to correct shape mis-modeling.

Observation of the EWK diboson production

with a high-mass dijet system in semi-leptonic final states

EWK Measurements (7.4/6.0 observed/expected [σ])

	Combined	0-lepton	1-lepton	2-lepton	Resolved	Merged
$\sigma^{fid,exp}_{EWK,V_{lep}V_{had}jj}$	22.9 fb	7.3 fb	12.0 fb	3.6 fb	12.4 fb	10.5 fb
$\sigma^{fid,obs}_{EWK,V_{lep}V_{had}jj}$	33.0 ± 5.5 fb	15.8 ± 2.9 fb	12.5 ± 3.2 fb	4.1 ± 1.5 fb	19.1 ± 4.6 fb	13.8 ± 4.1 fb

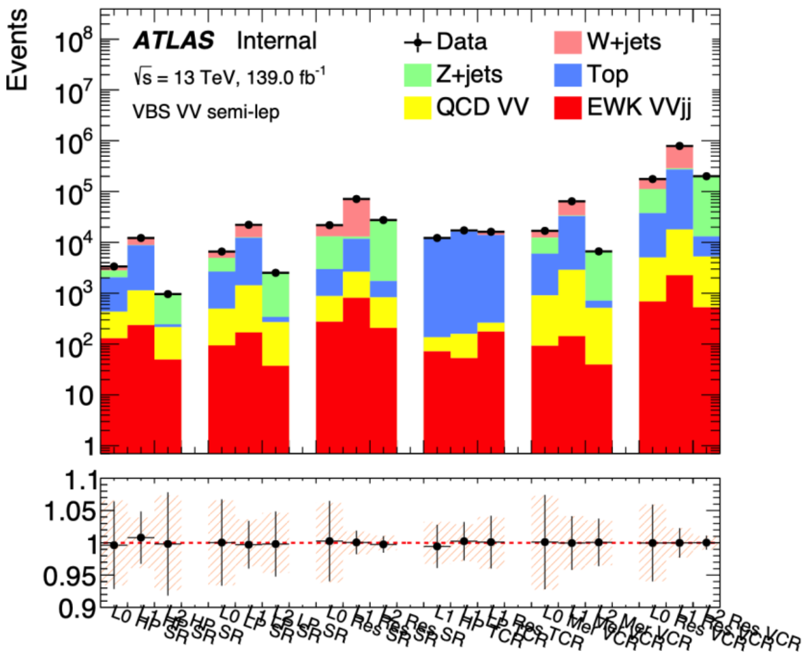

Uncertainty source	σ_μ
Total uncertainty	0.218
Statistical	0.093
Systematic	0.197
Theoretical and modeling uncertainties	
Floating normalizations	0.038
Z + jets	0.061
W + jets	0.068
$t\bar{t}$	0.016
Diboson	0.045
single-top	0.009
Signal Modelling	0.126
MC statistics	0.073
Experimental uncertainties	
Jets and E_T^{miss}	0.088
Leptons	0.005
b-tagging	0.004
Luminosity	0.023
m_{jj}^{tag} reweighting	0.063

EWK QCD simultaneously fit

At the reconstructed level, the interference term results in a 5% (20%) uncertainty on the RNN distribution in the resolved (merged) signal regions.

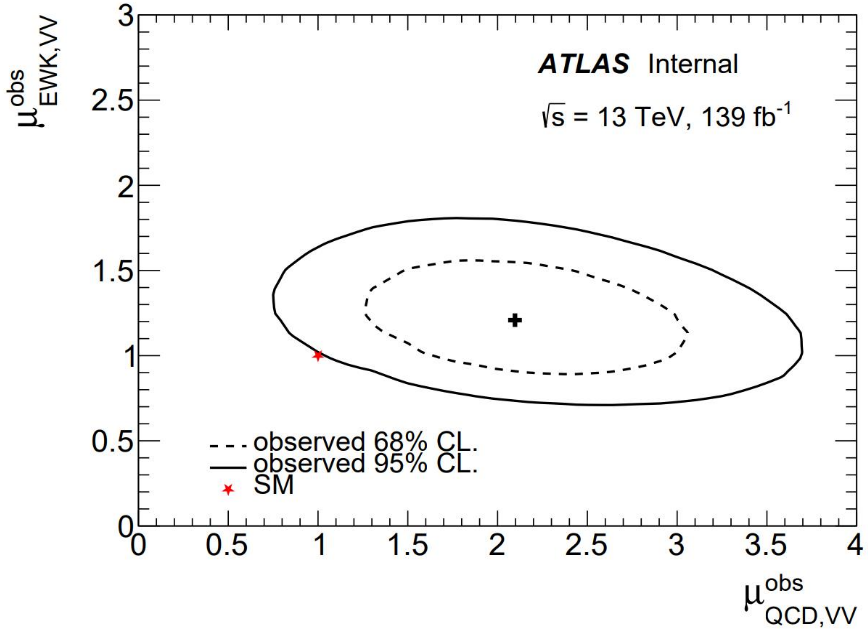

Observation of the EWK diboson production
with a high-mass dijet system in semi-leptonic final states

EFT interpretations

Eboli model is used, **19** of the 21 operators affect the semi-leptonic final states.

The total matrix element with the addition of new dimension-8 operators can be written as:

$$|A_{SM} + \frac{f_i}{\Lambda^4} A_i| = |A_{SM}^2| + \sum_i \frac{f_i^2}{\Lambda^8}|A_i^2| + \sum_i 2\frac{f_i}{\Lambda^4}\mathrm{Re}(A_{SM}^\star A_i) + \sum_{i \neq j} \frac{f_i}{\Lambda^4}\frac{f_j}{\Lambda^4}\mathrm{Re}(A_i^\star A_j)$$

The possible interference terms between EFT operators are not considered in this result.

Wilson Coefficient	Expected limit	Observed Limit
f_{T0}/Λ^4	[-0.20, 0.18]	[-0.25, 0.22]
f_{T1}/Λ^4	[-0.19, 0.19]	[-0.24, 0.24]
f_{T2}/Λ^4	[-0.44, 0.45]	[-0.56, 0.56]
f_{T5}/Λ^4	[-0.57, 0.53]	[-0.64, 0.59]
f_{T6}/Λ^4	[-0.76, 0.72]	[-0.74, 0.72]
f_{T7}/Λ^4	[-1.78, 1.57]	[-1.96, 1.72]
f_{T8}/Λ^4	[-0.59, 0.59]	[-0.48, 0.48]
f_{T9}/Λ^4	[-1.22, 1.22]	[-1.03, 1.04]
f_{S02}/Λ^4	[-3.22, 3.23]	[-3.92, 3.93]
f_{S1}/Λ^4	[-6.86, 6.88]	[-7.90, 7.87]
f_{M0}/Λ^4	[-1.13, 1.13]	[-1.27, 1.27]
f_{M1}/Λ^4	[-3.24, 3.24]	[-3.97, 3.98]
f_{M2}/Λ^4	[-1.66, 1.67]	[-1.86, 1.86]
f_{M3}/Λ^4	[-5.29, 5.29]	[-5.74, 5.75]
f_{M4}/Λ^4	[-2.62, 2.62]	[-2.99, 2.99]
f_{M5}/Λ^4	[-3.81, 3.84]	[-4.45, 4.48]
f_{M7}/Λ^4	[-5.33, 5.21]	[-6.65, 6.48]

Measurements of the EWK $W^{\pm}Z$ pair production

in association with two jets (Arxiv)

Signal: EWK $WZjj$
Background:
- Irreducible: ZZ, $t\bar{t}$+V --> ZZ-CR, b-CR
- reducible: Z+j, Zγ, $t\bar{t}$, Wt, WW --> data-driven estimation

	SR, $N_{\text{jets}} = 2$	SR, $N_{\text{jets}} \geq 3$	b-CR	ZZ-CR
Data	169	477	666	210
Total pred.	231 ± 12	550 ± 50	660 ± 40	205 ± 11
$WZjj$-EW	65.0 ± 3.5	60 ± 6	4.82 ± 0.28	0.725 ± 0.014
$WZjj$-QCD	125 ± 9	380 ± 50	77 ± 18	6.2 ± 0.7
$WZjj$-INT	1.3 ± 0.6	5.3 ± 2.6	0.58 ± 0.29	0.22 ± 0.11
$t\bar{t}+V$	0.66 ± 0.04	20.2 ± 0.7	289 ± 10	9.89 ± 0.28
tZj	8.78 ± 0.34	19.7 ± 1.2	134 ± 4	0.432 ± 0.005
ZZ-QCD	9.6 ± 0.4	32.0 ± 2.5	10.1 ± 0.6	159 ± 9
ZZ-EW	2.2 ± 0.6	4.4 ± 1.1	0.25 ± 0.06	23 ± 6
VVV	0.41 ± 0.10	2.0 ± 0.5	0.39 ± 0.10	4.1 ± 1.1
Misid. leptons	18 ± 4	28 ± 7	150 ± 40	1.7 ± 0.5

Reconstruction -- 'resonant shape' algorithm

$$P = \left| \frac{1}{m^2_{(\ell^+,\ell^-)} - \left(m_Z^{\text{PDG}}\right)^2 + \mathrm{i}\,\Gamma_Z^{\text{PDG}}\, m_Z^{\text{PDG}}} \right|^2 \times \left| \frac{1}{m^2_{(\ell',\nu_{\ell'})} - \left(m_W^{\text{PDG}}\right)^2 + \mathrm{i}\,\Gamma_W^{\text{PDG}}\, m_W^{\text{PDG}}} \right|^2$$

The final choice of which leptons are assigned to the W or Z bosons corresponds to the configuration exhibiting the largest value of the estimator P.

- In this paper, both **integrated** and **differential** cross-sections are measured for EWK WZ and inclusive WZ both.
- A BDT is trained and optimized on simulated events from the SR to separate WZjj−EW events from all other processes.

Measurements of the EWK $W^{\pm}Z$ pair production

in association with two jets

Integrated cross-section measurement

$$\sigma_{WZjj\text{-EW}} = \sum_{i=1}^{2} \mu^i_{WZjj\text{-EW}} \cdot \sigma^{i,\,\text{th. MC}}_{WZjj\text{-EW}}\,,$$

$$\sigma_{WZjj\text{-strong}} = \sum_{i=1}^{2} \left(\mu^i_{WZjj\text{-QCD}} \cdot \sigma^{i,\,\text{th. MC}}_{WZjj\text{-QCD}} + \mu^i_{WZjj\text{-INT}} \cdot \sigma^{i,\,\text{th. MC}}_{WZjj\text{-INT}}\right)\,,$$

$$= \sum_{i=1}^{2} \left(\mu^i_{WZjj\text{-QCD}} \cdot \sigma^{i,\,\text{th. MC}}_{WZjj\text{-QCD}} + \sqrt{\mu^i_{WZjj\text{-EW}}} \cdot \sqrt{\mu^i_{WZjj\text{-QCD}}} \cdot \sigma^{i,\,\text{th. MC}}_{WZjj\text{-INT}}\right)$$

Results

$$\sigma_{WZjj\text{-EW}} = 0.368 \pm 0.037\,(\text{stat.}) \pm 0.059\,(\text{syst.}) \pm 0.003\,(\text{lumi.})\text{ fb}$$
$$= 0.37 \pm 0.07\text{ fb},$$
$$\sigma_{WZjj\text{-strong}} = 1.093 \pm 0.066\,(\text{stat.}) \pm 0.131\,(\text{syst.}) \pm 0.009\,(\text{lumi.})\text{ fb}$$
$$= 1.09 \pm 0.14\text{ fb},$$

Predictions from MadGraph+PYTHIA8

$$\sigma^{\text{MadGraph+Pythia8}}_{WZjj\text{-EW}} = 0.370 \pm 0.001\,(\text{stat.}) \pm 0.006\,(\text{PDF})\,^{+0.030}_{-0.026}\,(\text{scale})\text{ fb}\,,$$
$$\sigma^{\text{MadGraph+Pythia8}}_{WZjj\text{-strong}} = 1.537 \pm 0.009\,(\text{stat.}) \pm 0.016\,(\text{PDF})\,^{+0.087}_{-0.149}\,(\text{scale})\text{ fb}\,,$$

Systematic uncertainties

Source	$\frac{\Delta\sigma_{WZjj\text{-EW}}}{\sigma_{WZjj\text{-EW}}}$ [%]	$\frac{\Delta\sigma_{WZjj\text{-strong}}}{\sigma_{WZjj\text{-strong}}}$ [%]
$WZjj$–EW theory modelling	7	1.8
$WZjj$–QCD theory modelling	2.8	8
$WZjj$–EW and $WZjj$–QCD interference	0.35	0.6
PDFs	1.0	0.06
Jets	2.3	5
Pile-up	1.1	0.6
Electrons	0.8	0.8
Muons	0.9	0.9
b-tagging	0.10	0.11
MC statistics	1.9	1.2
Misid. lepton background	2.3	2.3
Other backgrounds	0.9	0.23
Luminosity	0.7	0.9
All systematics	16	12
Statistics	10	6
Total	19	13

Measurements of the EWK $W^{\pm}Z$ pair production

in association with two jets

Differential cross-section measurement

$$\sigma^{i}_{WZjj-\mathrm{EW}} = \mu^{i}_{WZjj-\mathrm{EW}} \cdot \sigma^{i,\,\mathrm{th.\,MC}}_{WZjj-\mathrm{EW}} = \frac{N^{i}_{\mathrm{fit}}}{\mathcal{L} \cdot C_i}, \quad C_i = \frac{N^{i}_{\mathrm{MC,\,det.}}}{N^{i}_{\mathrm{MC,\,part.}}}$$

C_i is a bin-by-bin correction factor for detector inefficiency, resolution and bin-to-bin migrations.

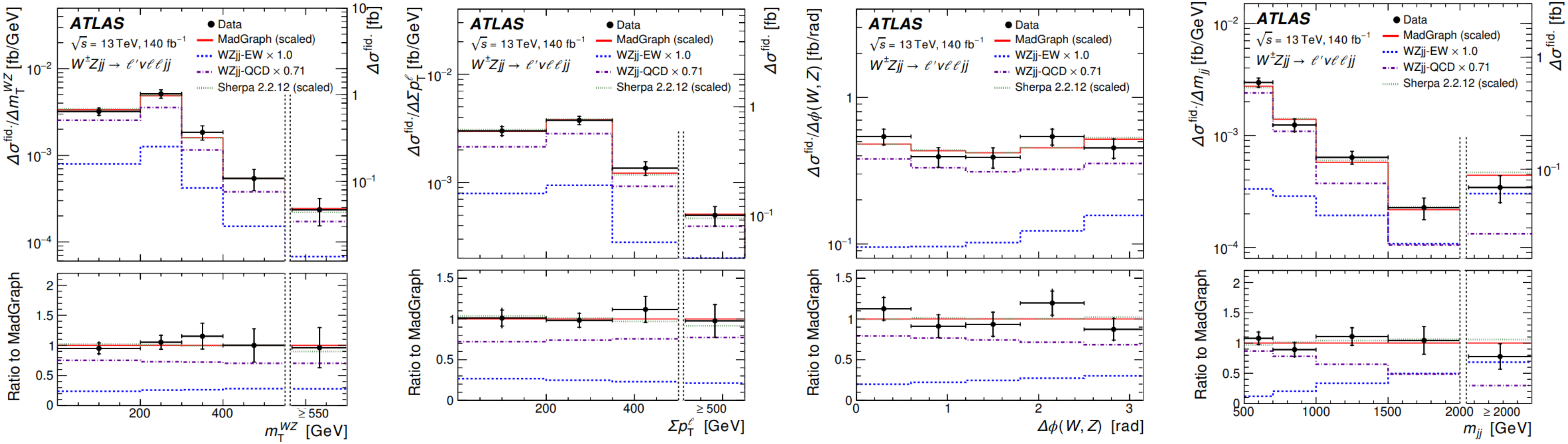

Measurements of the ZZ production

in the four-lepton final state (Arxiv)

Signal: $q\bar{q} \rightarrow ZZ, gg \rightarrow ZZ, qq \rightarrow ZZ + 2j$

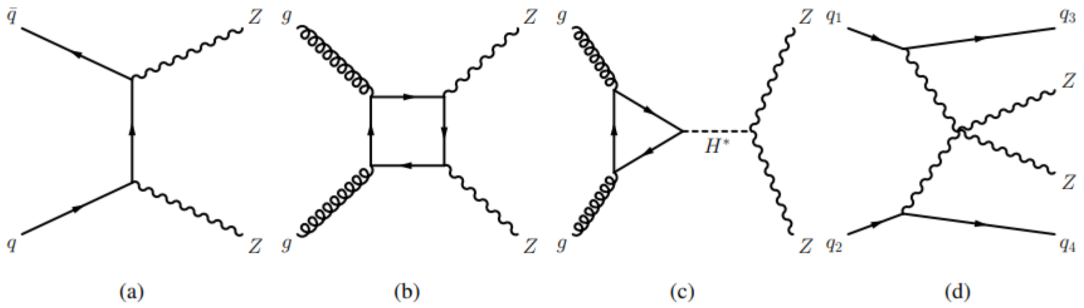

Background: $t\bar{t}Z, VVV$, other reducible backgrounds

This analysis uses pp collision data recorded by the ATLAS detector in 2022, the first year of the Run 3 data taking period.

Signal region kinematic distributions. Data are compared with the predictions with all uncertainties included.

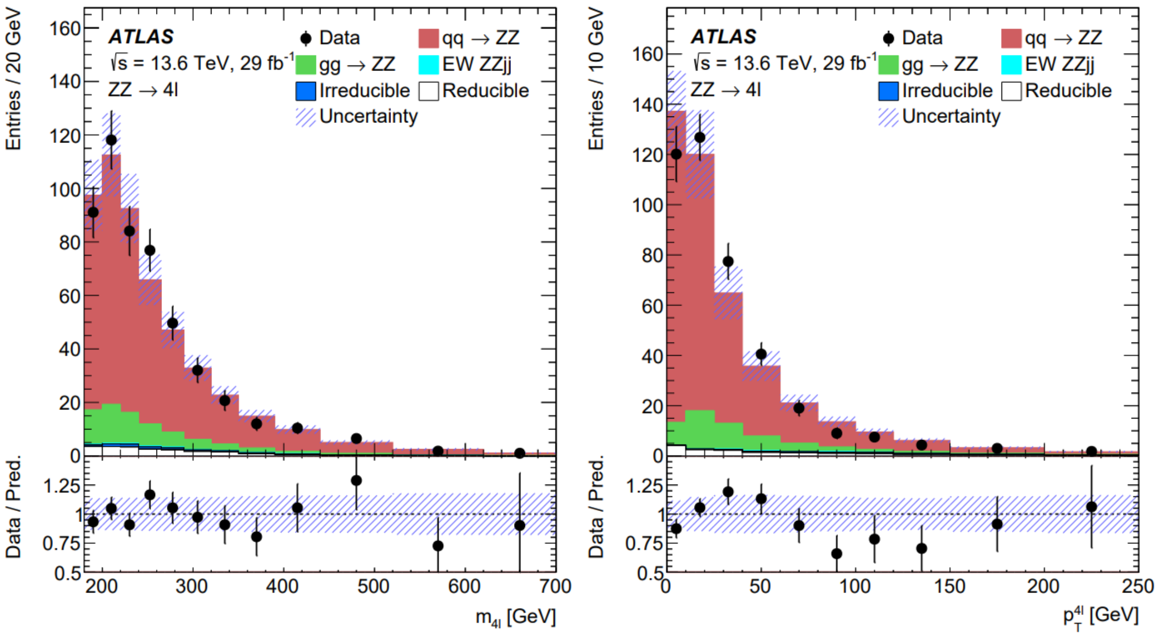

The Observed and predicted detector level yields in the SR

Process	$q\bar{q} \rightarrow ZZ$	$gg \rightarrow ZZ$	EW $qq \rightarrow ZZ + 2j$	$t\bar{t}Z$	VVV	Reducible	Total	Data
Yield	515 ± 50	74 ± 44	4.7 ± 1.0	5.5 ± 0.8	2.1 ± 0.2	25.4 ± 8.1	626 ± 88	625

Measurements of the ZZ production

in the four-lepton final state (Arxiv)

The inclusive cross-section in the fiducial region is calculated as:

$$\sigma_{\text{fid}} = \frac{N_{\text{obs}} - N_{\text{bkg}}}{L \times C_{ZZ}}$$

And it's measured to be:

$$\sigma_{\text{fid}} = 36.7 \pm 1.6(\text{stat}) \pm 1.5(\text{syst}) \pm 0.8(\text{lumi}) \text{ fb}$$

Source	Relative uncertainty(%)
Data statistical uncertainty	4.2
MC statistical uncertainty	0.3
Luminosity	2.2
Pile-up	0.3
Lepton momentum	0.2
Lepton efficiency	3.7
Background	1.6
Theoretical uncertainty	1.0
Total	6.3

The measured differential cross-sections (filled points) are compared with the predictions in each bins.

- error bars give the total uncertainty
- the hatched band gives the systematic uncertainty

MATRIX calculates $gg \rightarrow ZZ$ at NLO QCD accuracy. Only the QCD scale uncertainty is considered in the MATRIX predictions.

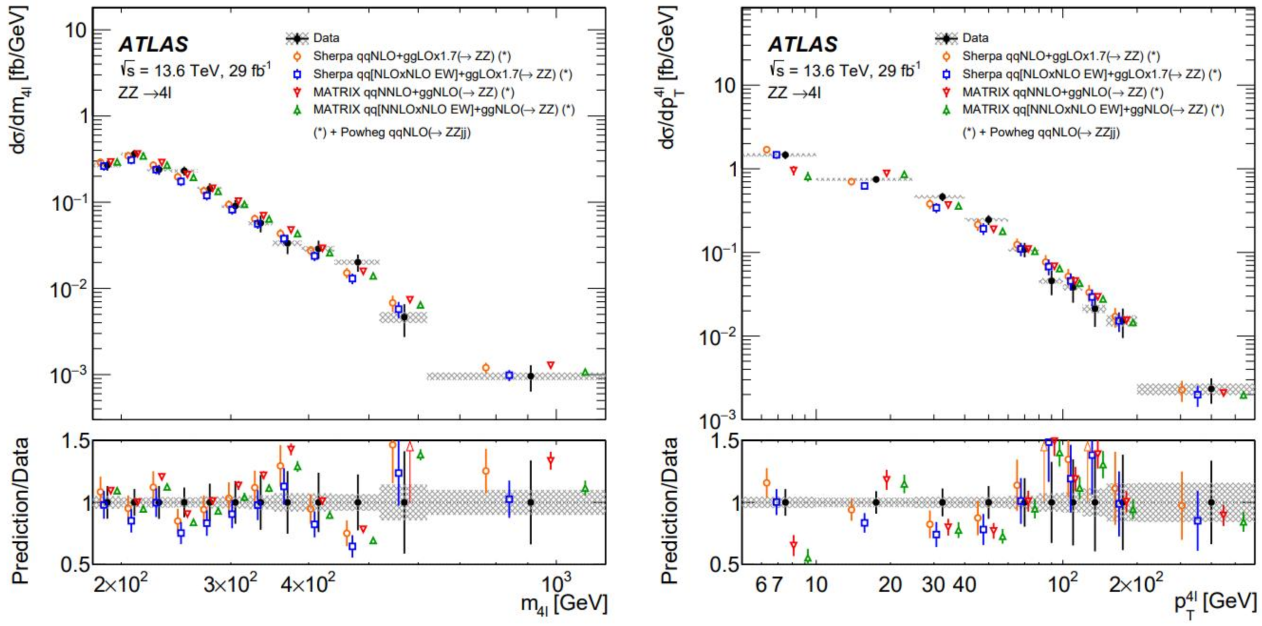

(a) (b)

Measurements of the EWK $W^{\pm}\gamma$ pair production

in association with two jets (EPJC)

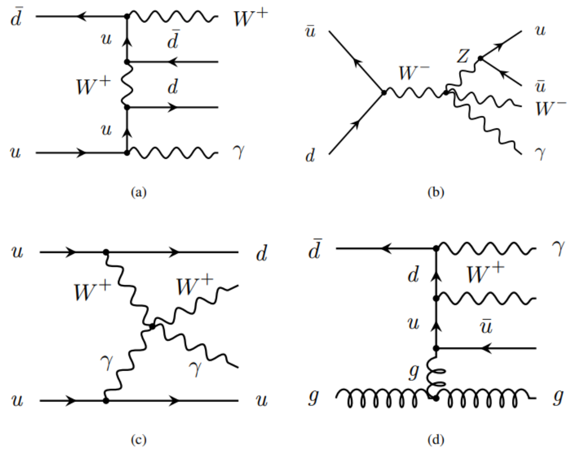

Signal: EWK $W\gamma jj$

Dominant Background: Strong $W\gamma jj$

	$\mathrm{SR^{fid}}\left(N_{\mathrm{jets}}^{\mathrm{gap}}=0\right)$	$\mathrm{CR^{fid}}\left(N_{\mathrm{jets}}^{\mathrm{gap}}>0\right)$
EW $W\gamma jj$	520 ± 141	120 ± 49
Strong $W\gamma jj$	1550 ± 830	1970 ± 950
Non-prompt	692 ± 57	698 ± 58
Top quark processes	109 ± 18	183 ± 37
EW + strong $Z\gamma jj$	128 ± 34	163 ± 77
Total	3000 ± 830	3140 ± 960
Data	3341	3143

The differential cross-sections for EWK $W\gamma jj$ are measured as functions of two types of variables:

- VBS observables
- charge conjugation and parity (CP) observables.

The **signal and control regions** are defined as:

Fiducial cross-section	$\mathrm{SR^{fid}}$		$\mathrm{CR^{fid}}$	
	$N_{\mathrm{jets}}^{\mathrm{gap}}=0$		$N_{\mathrm{jets}}^{\mathrm{gap}}>0$	
Differential cross-section	SR	$\mathrm{CR_A}$	$\mathrm{CR_B}$	$\mathrm{CR_C}$
$m_{jj}>1$ TeV	$N_{\mathrm{jets}}^{\mathrm{gap}}=0$ $\xi_{l\gamma}<0.35$	$N_{\mathrm{jets}}^{\mathrm{gap}}>0$ $\xi_{l\gamma}<0.35$	$N_{\mathrm{jets}}^{\mathrm{gap}}>0$ $0.35<\xi_{l\gamma}<1$	$N_{\mathrm{jets}}^{\mathrm{gap}}=0$ $0.35<\xi_{l\gamma}<1$

Where,

$$\xi_{l\gamma}=\left|\left(y_{l\gamma}-(y_{j_1}+y_{j_2})/2\right)/(y_{j_1}-y_{j_2})\right|$$

Measures The centrality of the lepton-photon system relative to the VBS tagged jets

Measurements of the EWK $W^{\pm}\gamma$ pair production

in association with two jets (EPJC)

Post-fit plots of SR and CR

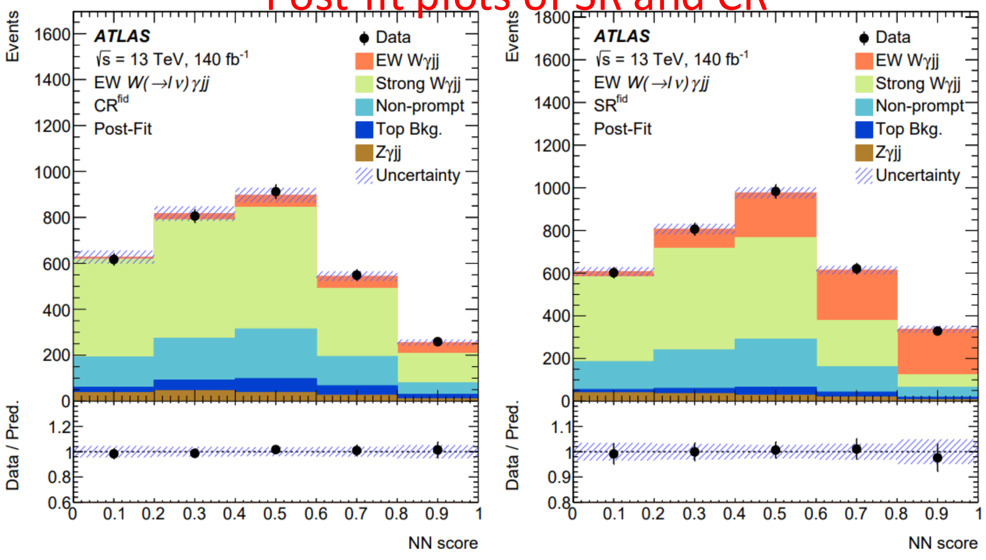

Uncertainty Source	Fractional Uncertainty [%]
MC Statistics	11
Jets	8
Lepton, photon, pile-up	8
EW $W\gamma jj$ modelling	7
Data Statistics	6
Strong $W\gamma jj$ modelling	6
Non-prompt background	2
Luminosity	2
Other Background modelling	2
E_T^{miss}	1

The measured EW $W\gamma jj$ fiducial cross-section compared with the predictions of SHERPA and MADGRAPH5+PYTHIA8

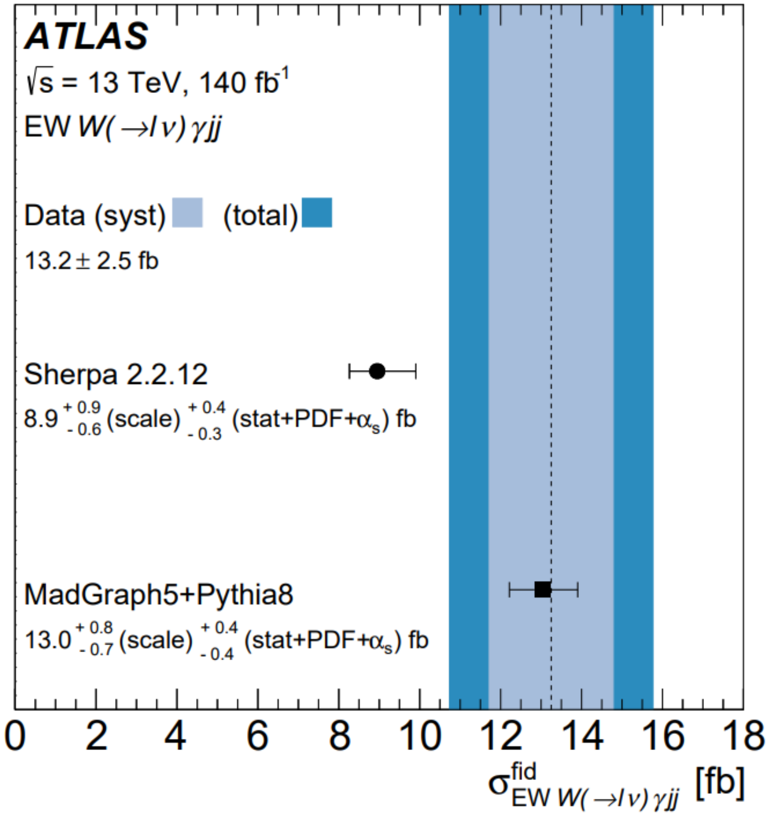

The difference between the predicted cross-section between MadGraph5+Pythia8 and Sherpa arises due to the third parton included in the matrix element of Sherpa. arxiv

Differential cross section and EFT

Expected and observed 95% CL limits for specified $m_{W\gamma}$ cut-off values, where the expected limit for some operators intersects with the unitarity bounds derived from partial wave unitarity constraints. Note "-" is used in the column for those operators that do not cross the unitarity bound over the range of the clipping scan

Coefficients [TeV^{-4}]	Observable	$M_{W\gamma}$ cut-off [TeV]	Expected [TeV^{-4}]	Observed [TeV^{-4}]
f_{T0}/Λ^4	p_T^{jj}	-	[-2.4,2.4]	[-1.7,1.8]
f_{T1}/Λ^4	p_T^{jj}	-	[-1.5,1.6]	[-1.1,1.2]
f_{T2}/Λ^4	p_T^{jj}	-	[-4.4,4.7]	[-3.1,3.5]
f_{T3}/Λ^4	p_T^{jj}	-	[-3.3,3.5]	[-2.4,2.6]
f_{T4}/Λ^4	p_T^{jj}	-	[-3.0,3.0]	[-2.2,2.2]
f_{T5}/Λ^4	p_T^{jj}	1.1	[-9.9,9.9]	[-7.5,7.5]
f_{T6}/Λ^4	p_T^{jj}	1.3	[-7.4,7.6]	[-5.2,5.4]
f_{T7}/Λ^4	p_T^{jj}	-	[-3.8,3.9]	[-2.7,2.8]
f_{M0}/Λ^4	p_T^{l}	-	[-38,37]	[-38,37]
f_{M1}/Λ^4	p_T^{l}	-	[-57,58]	[-41,42]
f_{M2}/Λ^4	p_T^{l}	0.8	[-110,110]	[-88,82]
f_{M3}/Λ^4	p_T^{l}	1.1	[-100,110]	[-73,77]
f_{M4}/Λ^4	p_T^{l}	1.0	[-118,111]	[-89,83]
f_{M5}/Λ^4	p_T^{l}	1.3	[-57,80]	[-32,77]
f_{M7}/Λ^4	p_T^{l}	-	[-96,95]	[-69,68]

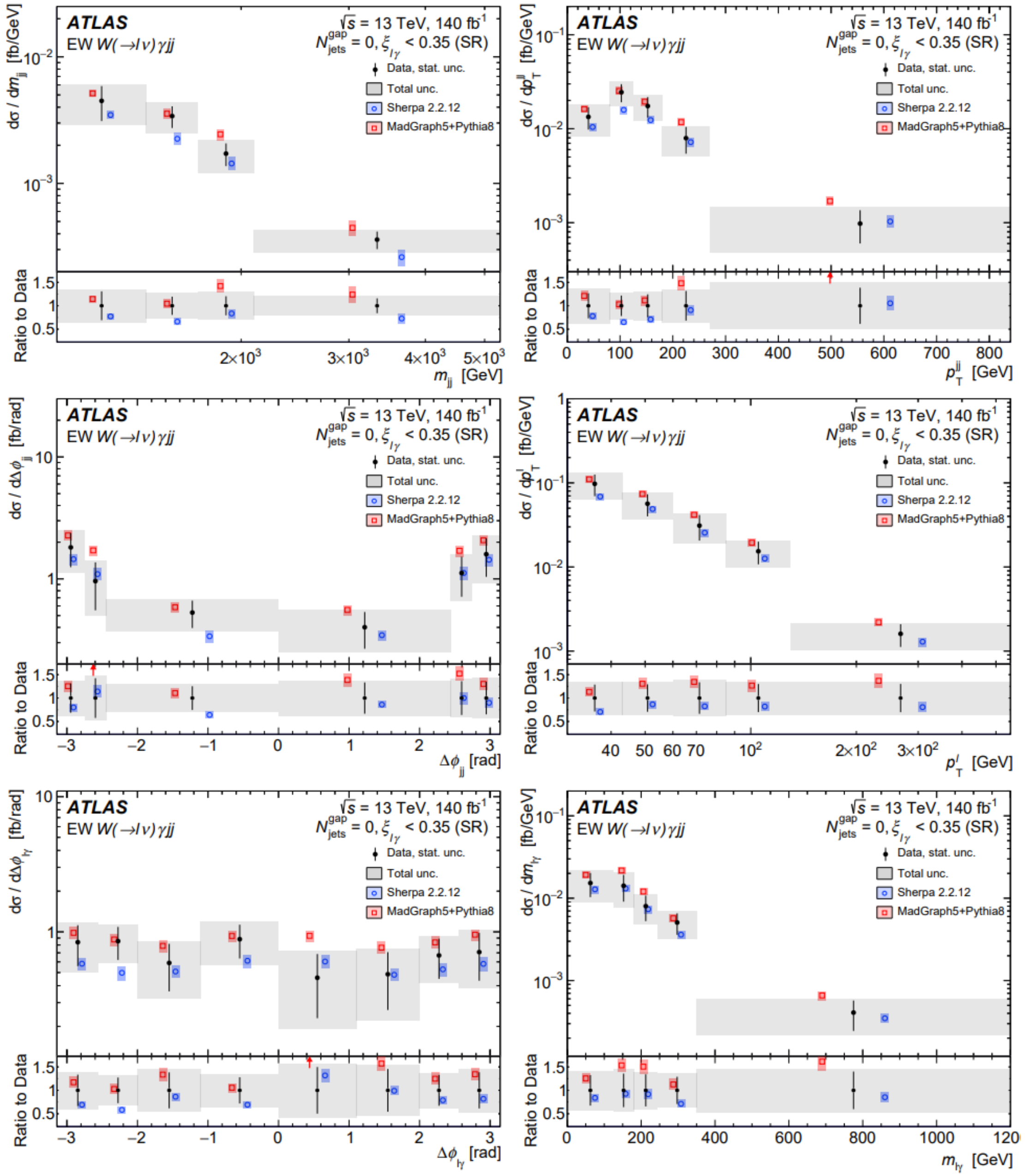

WZ polarization and Radiation Amplitude Zero effect

(Arxiv)

- **Radiation Amplitude Zero(RAZ) effect**: The dominant helicity amplitude with two **transversely-polarized** bosons is exactly **zero** when the scattering angle of the W boson in the WZ rest frame with respect to the incoming antiquark direction approaches **90 degrees**, which is from the gauge structure of SM.
- The RAZ effect will leads to a dip around 0 in the $\Delta Y(WZ)$ and $\Delta Y(\ell_W Z)$ distributions for TT (transverse transverse) component of WZ production process.
- The other components are subtracted from data, an iterative Bayesian **unfolding** method is used to correct the detector effects

Process	$100 < p_T^Z \leq 200$ GeV	$p_T^Z > 200$ GeV
W_0Z_0	222 ± 5	47.6 ± 1.5
$W_0Z_T + W_TZ_0$	323 ± 12	23.7 ± 0.8
W_TZ_T	856 ± 31	124 ± 4
Prompt background	169 ± 18	24.1 ± 2.7
Non-prompt background	68 ± 29	2.8 ± 1.1
Total Expected	1640 ± 60	222 ± 8
Data	1740	236

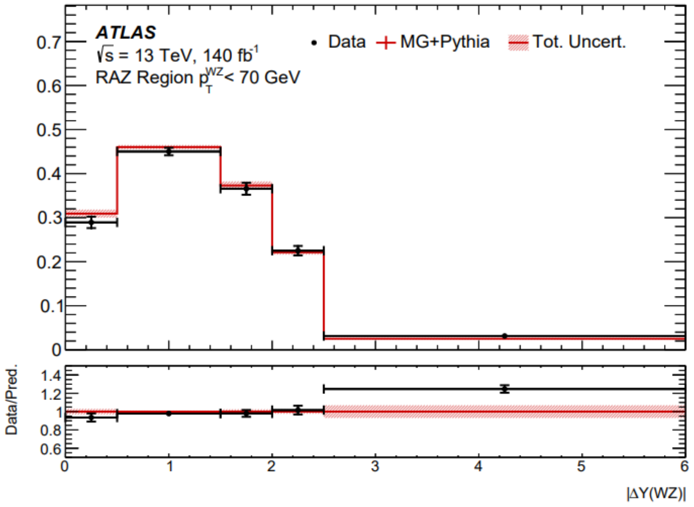

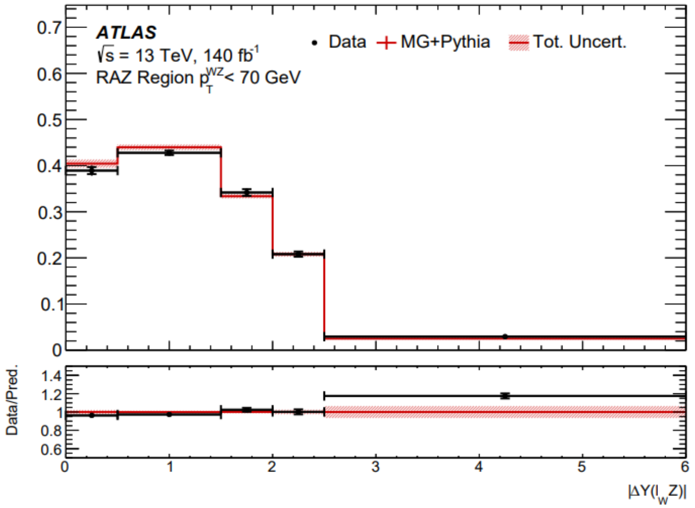

WZ polarization and Radiation Amplitude Zero effect

(Arxiv)

Diboson polarization fractions are measured in two regions enhanced in events with 00 polarization:

- $p_T^{WZ} < 70$ GeV
- $100 < p_T^Z \leq 200$ GeV or $p_T^Z > 200$ GeV

BDTs are trained to further separate the 00 component from other components and backgrounds

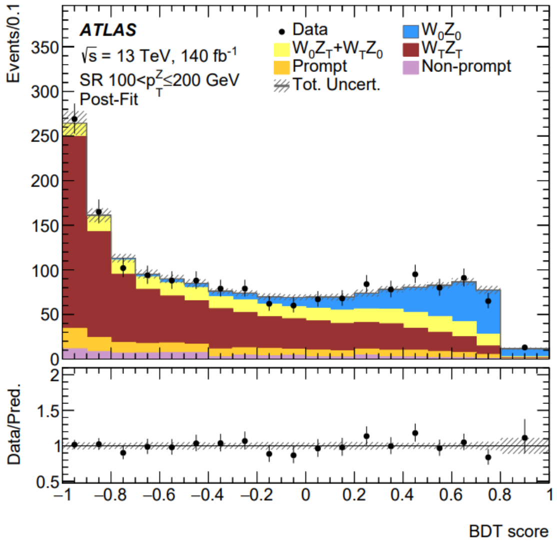

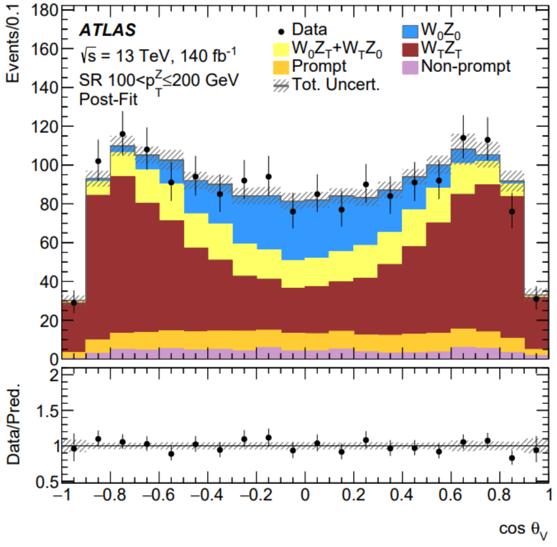

Diboson polarization fractions are measured in two signal regions with enhanced longitudinal polarization for both bosons

	Measurement			Prediction	
	$100 < p_T^Z \leq 200$ GeV	$p_T^Z > 200$ GeV		$100 < p_T^Z \leq 200$ GeV	$p_T^Z > 200$ GeV
f_{00}	$0.19 \pm^{0.03}_{0.03}$ (stat) $\pm^{0.02}_{0.02}$ (syst)	$0.13 \pm^{0.09}_{0.08}$ (stat) $\pm^{0.02}_{0.02}$ (syst)	f_{00}	0.152 ± 0.006	0.234 ± 0.007
f_{0T+T0}	$0.18 \pm^{0.07}_{0.08}$ (stat) $\pm^{0.05}_{0.06}$ (syst)	$0.23 \pm^{0.17}_{0.18}$ (stat) $\pm^{0.06}_{0.10}$ (syst)	f_{0T}	0.120 ± 0.002	0.062 ± 0.002
f_{TT}	$0.63 \pm^{0.05}_{0.05}$ (stat) $\pm^{0.04}_{0.04}$ (syst)	$0.64 \pm^{0.12}_{0.12}$ (stat) $\pm^{0.06}_{0.06}$ (syst)	f_{T0}	0.109 ± 0.001	0.058 ± 0.001
f_{00} obs (exp) sig.	5.2 (4.3) σ	1.6 (2.5) σ	f_{TT}	0.619 ± 0.007	0.646 ± 0.008

Evidence of pair production of longitudinally polarized vector bosons of ZZ (Arxiv)

BDT train for LL component selection

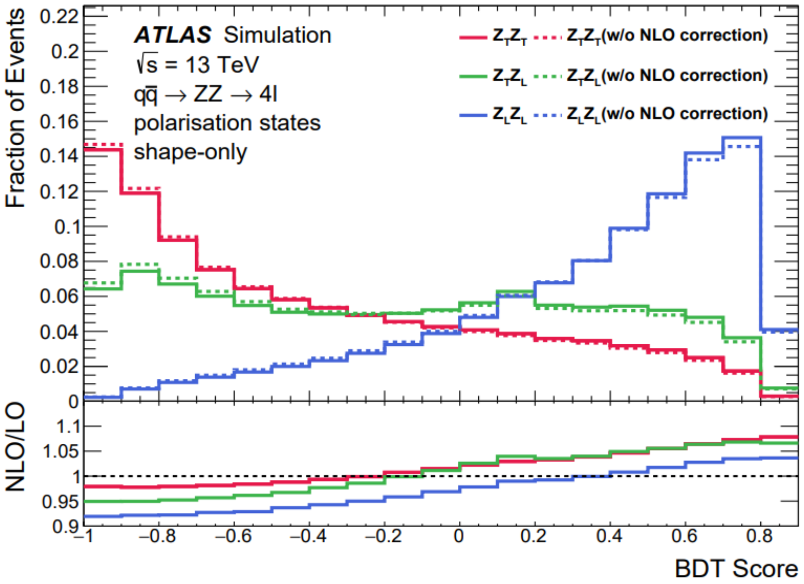

Pre- and post-fit expected and observed yield

		Pre-fit	Post-fit
ZZ	Z_LZ_L	189.3 ± 8.7	220 ± 54
	Z_TZ_L	710 ± 29	711 ± 29
	Z_TZ_T	2170 ± 120	2147 ± 60
	Interference	33.7 ± 2.8	33.4 ± 2.7
Non-prompt		18.7 ± 7.1	18.5 ± 7.0
Others		20.0 ± 3.7	19.9 ± 3.7
Total		3140 ± 150	3149 ± 57
Data		3149	3149

BDT post-fit

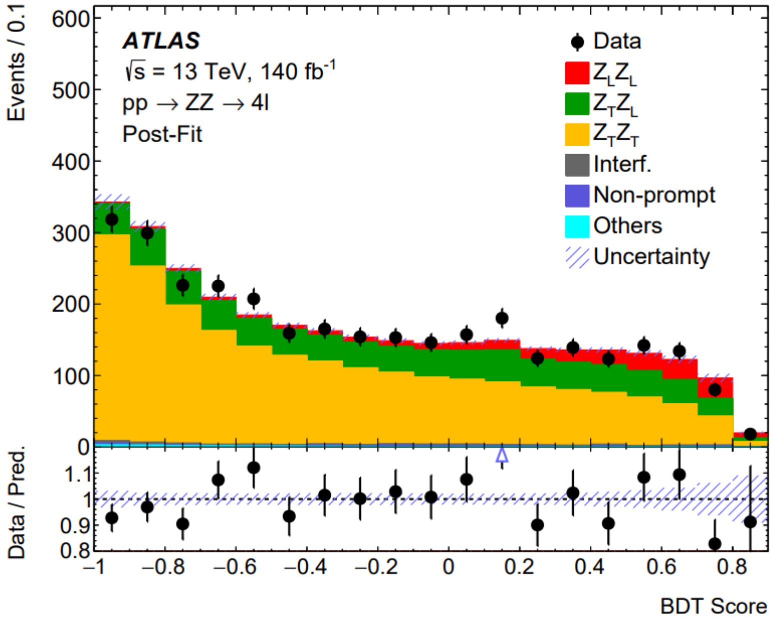

The measured LL component of ZZ is (4.3σ):

$$\mu_{LL} = 1.15 \pm 0.27(\text{stat.}) \pm 0.11(\text{syst.}) = 1.15 \pm 0.29$$

$$\sigma^{\text{obs.}}_{Z_LZ_L} = 2.45 \pm 0.56(\text{stat.}) \pm 0.21(\text{syst.})\ \text{fb}$$

Study of CP property of ZZ

(Arxiv)

To improve the sensitivity to detect the presence of a CP-odd aNTGC (anomalous neutral triple gauge couplings), an angular observable is formed to maximize the asymmetry for each Z-boson system:

$$T_{yz,1(3)} = \sin\phi_{1(3)} \times \cos\theta_{1(3)}$$

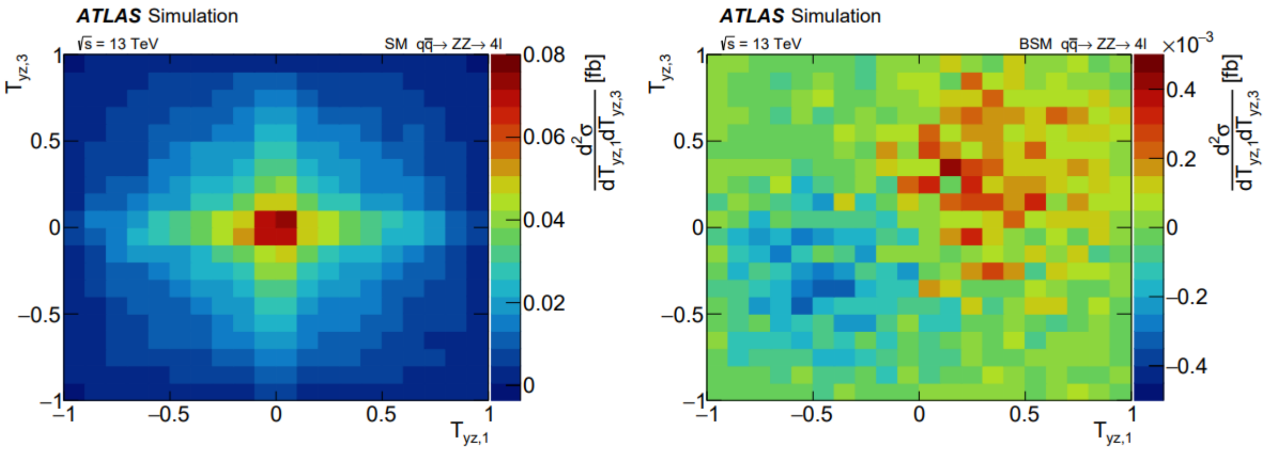

Particle level 2D differential cross-sections from SM prediction (left) and in the presence of the BSM aNTGC vertex (right).

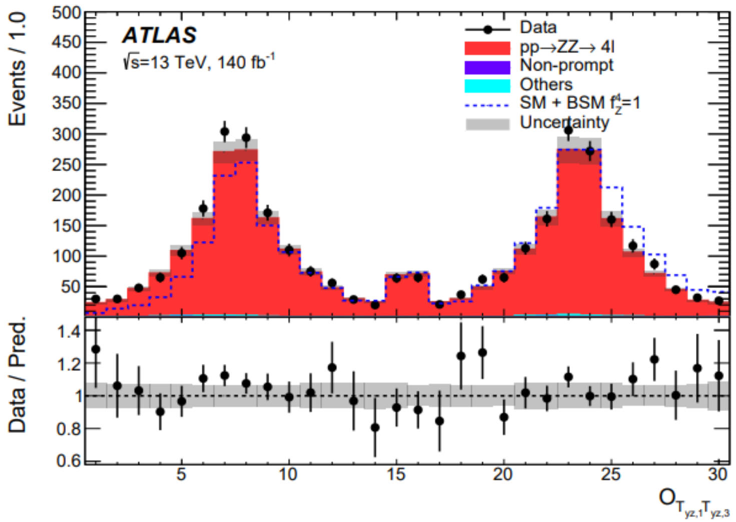

After $2D \rightarrow 1D$ mapping

Study of CP property of ZZ

(Arxiv)

Results

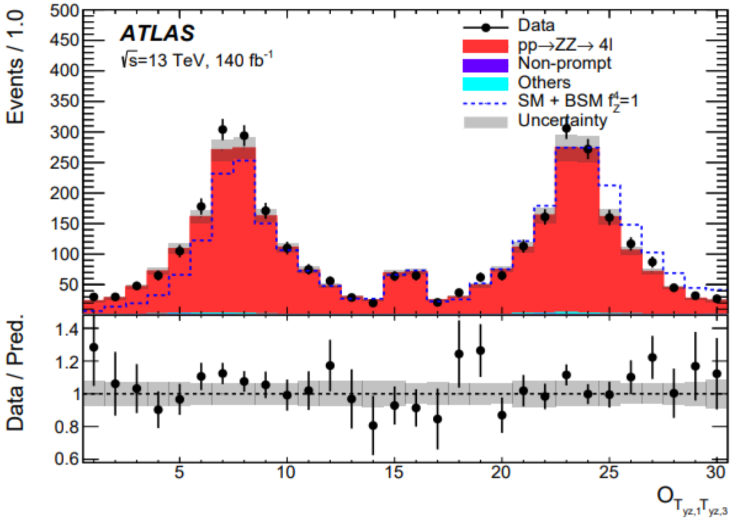

Expectation

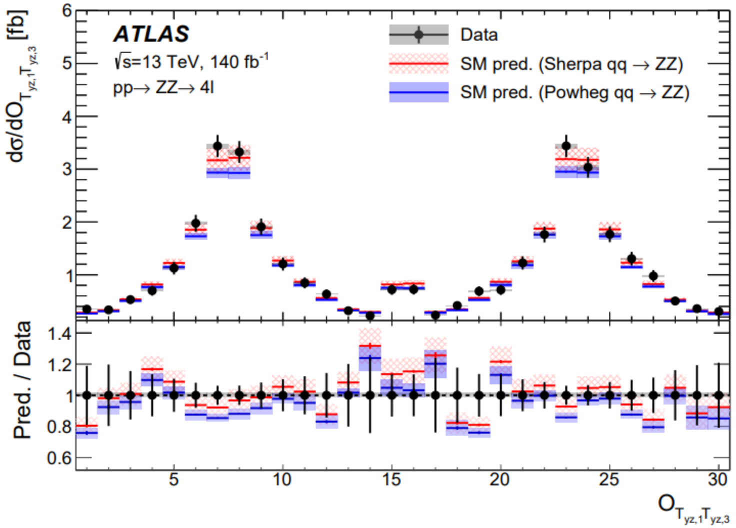

Measurement after unfolding

Contribution	Relative uncertainty [%]
Total	24
Data statistical uncertainty	23
Total systematic uncertainty	8.8
MC statistical uncertainty	1.7
Theoretical systematic uncertainties	
$q\bar{q} \to ZZ$ interference modelling	6.9
NLO reweighting observable choice for $q\bar{q} \to ZZ$	3.7
PDF, α_s and parton shower for $q\bar{q} \to ZZ$	2.2
NLO reweighting non-closure	1.0
QCD scale for $q\bar{q} \to ZZ$	0.2
NLO EW corrections for $q\bar{q} \to ZZ$	0.2
$gg \to ZZ$ modelling	1.4
Experimental systematic uncertainties	
Luminosity	0.8
Muons	0.6
Electrons	0.4
Non-prompt background	0.3
Pile-up reweighting	0.3
Triboson and $t\bar{t}Z$ normalisations	0.1

$WZ\gamma$ (PRL) and $W\gamma\gamma$ (inspire) observation

$WZ\gamma$ observation

Simultaneous fit with $\mu_{ZZ\gamma}, \mu_{ZZ}$;

$WZ\gamma$ observed with 6.3 σ

$$\sigma_{WZ\gamma} = 2.01 \pm 0.30 \text{ (stat.)} \pm 0.16 \text{ (syst.) fb}$$

Process	SR	$ZZ\gamma$ CR	$ZZ(e \to \gamma)$ CR
$WZ\gamma$	92 ± 15	0.21 ± 0.07	0.56 ± 0.14
$ZZ\gamma$	10.7 ± 2.3	23 ± 5	1.8 ± 0.4
$ZZ(e \to \gamma)$	3.0 ± 0.6	0.028 ± 0.020	30 ± 6
$Z\gamma\gamma$	1.05 ± 0.32	0.15 ± 0.06	0.29 ± 0.10
Fake background	30 ± 6	-	-
Pile-up γ	1.9 ± 0.7	-	-
Total predicted	139 ± 12	23 ± 5	33 ± 6
Data	139	23	33

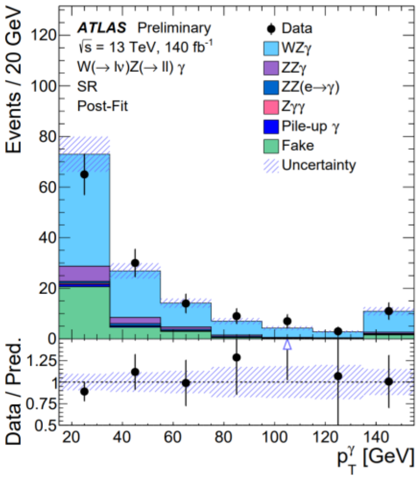

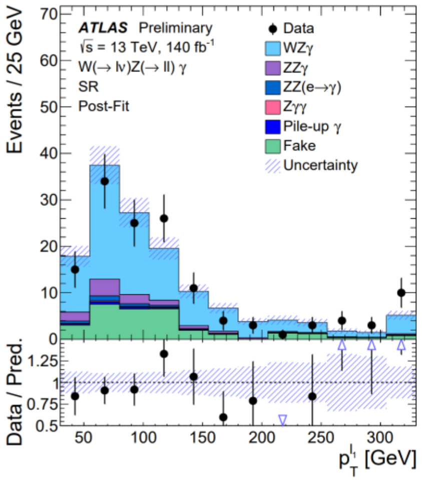

$W\gamma\gamma$ observation

data-driven Fake estimated in control regions

$WZ\gamma$ observed with 5.6 σ

$$\sigma_{fid} = 12.1^{+2.5}_{-2.2} \text{ fb}^{-1}$$

	SR	TopCR
$W\gamma\gamma$	410 ± 60	28 ± 5
Non-prompt $j \to \gamma$	420 ± 50	42 ± 20
Misidentified $e \to \gamma$	155 ± 11	120 ± 9
Multiboson ($WH(\gamma\gamma)$, $WW\gamma$, $Z\gamma\gamma$)	76 ± 13	5.2 ± 1.7
Non-prompt $j \to \ell$	35 ± 10	–
Top ($tt\gamma$, $tW\gamma$, $tq\gamma$)	30 ± 7	136 ± 32
Pileup	10 ± 5	–
Total	$1\,136 \pm 34$	332 ± 18
Data	$1\,136$	333

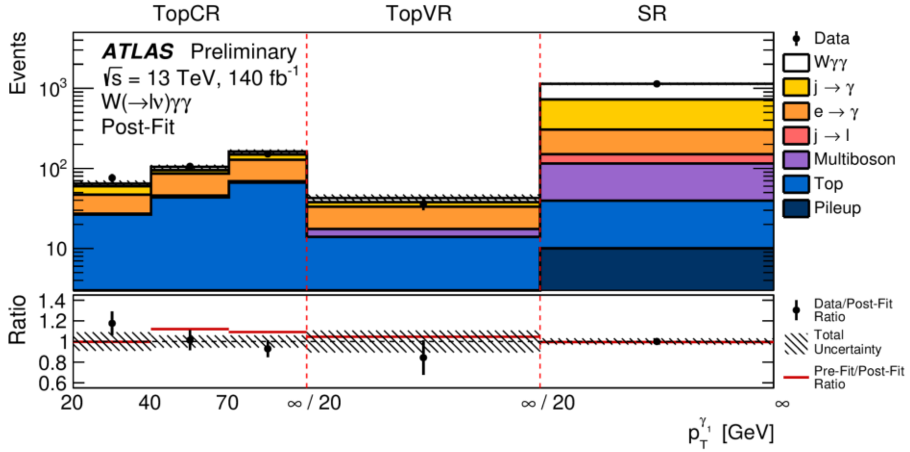

Summary

New multi-boson cross-section (integrated and differential) measurements of:

- EWK WZjj production
- ZZ production (Run 3 data)
- EWK Wγjj production

New evidence or observations @ATLAS:

- Observation of the EWK diboson production with a high-mass dijet system in semi-leptonic final states
- First Radiation Amplitude Zero effect in WZ production
- Evidence of pair production of longitudinally polarized vector bosons of ZZ
- Observation of $WZ\gamma$ production
- Observation of $W\gamma\gamma$ production

Each analysis includes EFT interpretations that can be included in the combinations in the future.

More challenges and opportunities in the future with more data and higher quality!

Backup

Measurements of the EWK $W^{\pm}Z$ pair production

in association with two jets

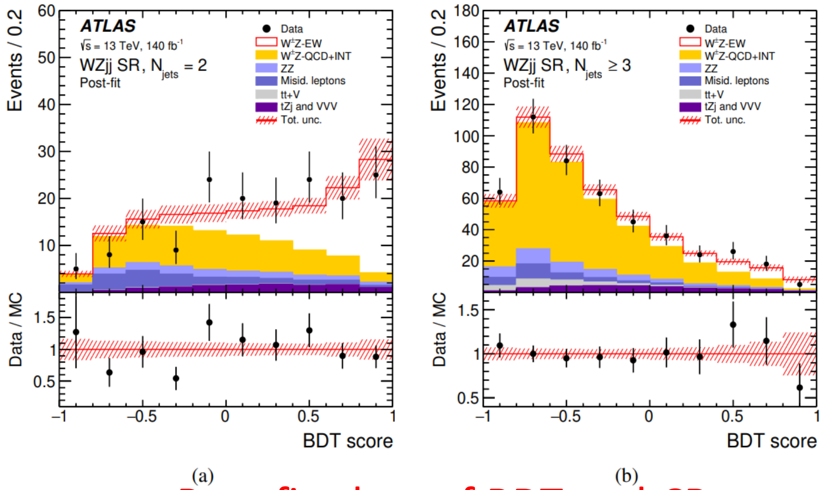

Post-fit plots of BDT and CR

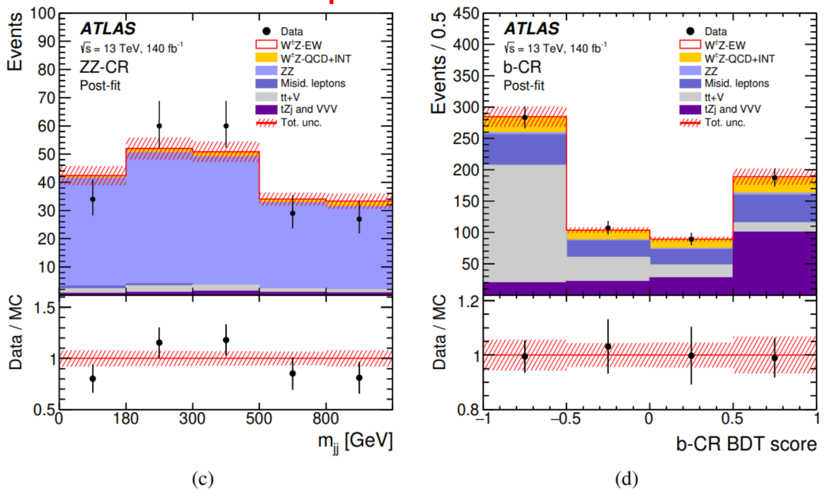

The measured WZjj−EW and WZjj−strong integrated cross-sections compared with predictions from MadGraph+PYTHIA8 and Sherpa 2.2.12